

Where is the level of neutral buoyancy for deep convection?

Hanii Takahashi¹ and Zhengzhao Luo²

Received 5 June 2012; revised 6 July 2012; accepted 9 July 2012; published 14 August 2012.

[1] This study revisits an old concept in meteorology - level of neutral buoyancy (LNB). The classic definition of LNB is derived from the parcel theory and can be estimated from the ambient sounding (LNB_sounding) without having to observe any actual convective cloud development. In reality, however, convection interacts with the environment in complicated ways; it will eventually manage to find its own effective LNB and manifests it through detraining masses and developing anvils (LNB_observation). This study conducts a near-global survey of LNB_observation for tropical deep convection using CloudSat data and makes comparison with the corresponding LNB_sounding. The principal findings are as follows: First, although LNB_sounding provides a reasonable upper bound for convective development, correlation between LNB_sounding and LNB_observation is low suggesting that ambient sounding contains limited information for accurately predicting the actual LNB. Second, maximum mass outflow is located more than 3 km lower than LNB_sounding. Hence, from convective transport perspective, LNB_sounding is a significant overestimate of the “destination” height level of the detrained mass. Third, LNB_observation is consistently higher over land than over ocean, although LNB_sounding is similar between land and ocean. This difference is likely related to the contrasts in convective strength and environment between land and ocean. Finally, we estimate the bulk entrainment rates associated with the observed deep convection, which can serve as an observational basis for adjusting GCM cumulus parameterization. **Citation:** Takahashi, H., and Z. Luo (2012), Where is the level of neutral buoyancy for deep convection?, *Geophys. Res. Lett.*, *39*, L15809, doi:10.1029/2012GL052638.

1. Introduction

[2] Level of neutral buoyancy (LNB) is a critical parameter for understanding convection because it sets the potential vertical extent for convective development. Occasionally, strong convective turrets overshoot the LNB and may even penetrate into the stratosphere. In this case, knowledge of LNB provides important information for defining the overshooting features.

[3] The classic definition of LNB is derived from the parcel theory by lifting a near-surface air parcel adiabatically to the upper troposphere where the air parcel starts to lose

buoyancy. It can be estimated from the ambient sounding without having to observe any actual convective cloud development. In reality, however, convection interacts with the environment in complicated ways and will eventually manage to find its own effective LNB where it ceases to ascend and starts to detrain masses. The parcel theory may not be able to accurately predict *a priori* the effective LNB for each individual convective cloud; only the convective cloud itself knows this level and will manifest it through the development of cirrus anvils.

[4] *Mullendore et al.* [2009] used a case study from the Tropical Rainfall Measuring Mission (TRMM) Large-scale Biosphere-Atmosphere (LBA) field campaign to show that the level of maximum detraining of an observed squall line (which can be interpreted as the cloud’s manifestation of the effective LNB) is significantly lower than the LNB derived from the sounding data. However, no global analysis has been done to generalize the conclusion. This present study corrects the situation by conducting a near-global survey of the effective LNB using satellite observations (LNB_observation hereafter) and comparing it to the LNB based on the ambient sounding (LNB_sounding hereafter). The difference between the two is indicative of the underlying convective processes (e.g., dilution from entrainment of environmental air). A near-global survey is an important first step to generalize our understanding of these processes and their regional variations.

[5] Previous studies used infrared brightness temperatures of the anvil clouds to estimate LNB [e.g., *Bedka et al.*, 2010]. This gives the uppermost level of the LNB. Analysis of CloudSat radar data, however, shows that anvil clouds develop over a thick layer of 4–5 km [e.g., *Cetrone and Houze*, 2009; *Yuan and Houze*, 2010]; within this thick layer, detrained masses are not uniformly distributed [*Yuan et al.*, 2011]. Further, *Mullendore et al.* [2009] found that radar reflectivity is well correlated with the convective mass detraining. Therefore, radar observations contain rich information concerning where convective updrafts lose buoyancy and transition to detraining and can thus be utilized to define LNB_observation in a more detailed manner than infrared brightness temperatures.

[6] A number of previous studies have used space-borne radars to characterize anvil cloud climatology and structures and relate them to the convective systems that produce them [*Cetrone and Houze*, 2009; *Yuan and Houze*, 2010; *Li and Schumacher*, 2011; *Yuan et al.*, 2011]. However, no attempt has been made to extract information on LNB and connect it to that based on sounding. The promising result from the case study by *Mullendore et al.* [2009] justifies a follow-up investigation of the problem using space-borne radar data. Here, we build upon these previous investigations and use CloudSat data to estimate LNB_observation and make comparison with LNB_sounding derived from collocated operational analysis. Compared to TRMM precipitation radar (PR),

¹Program in Earth and Environmental Sciences, Graduate Center, CUNY, New York, New York, USA.

²Department of Earth and Atmospheric Sciences and NOAA-CREST Center, City College of New York, CUNY, New York, New York, USA.

Corresponding author: Z. Luo, Department of Earth and Atmospheric Sciences, City College of New York, CUNY, New York, NY 10031, USA. (luo@sci.cuny.cuny.edu)

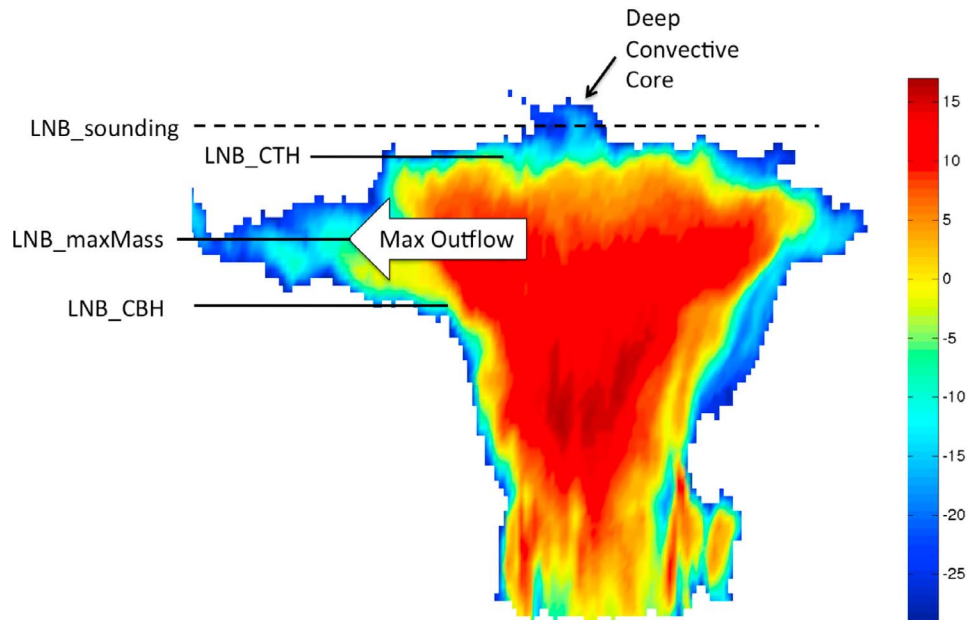


Figure 1. CloudSat radar reflectivity profile of a tropical deep convective cloud observed on February 24 2007 over Amazon (unit: dBZ). The size of the system is about 140 km and the highest point is about 17 km. Various forms of LNB_observation are marked up and illustrated using this example. LNB_CTH, LNB_maxMass and LNB_CBH refer to, respectively, LNB defined by anvil cloud top height (CTH), maximum mass outflow (determined by radar reflectivity) and anvil cloud base height (CBH). See text (the 4th paragraph of Section 2) for detailed explanation.

CloudSat cloud profiling radar (CPR) has higher sensitivity to non-precipitating particles and allows for a more complete depiction of the anvil structures [Yuan and Houze, 2010]. We focus on the tropics (30 S–30 N) in the present study but the analysis method could be expanded to mid-latitudes. The rest of the paper is organized as follows. Section 2 describes the analysis methods and data used. Results and interpretations are presented in Section 3. Section 4 summarizes the study.

2. Data and Analysis Methods

[7] CloudSat carries a 94-GHz, nadir-pointing, cloud profiling radar (CPR) sensitive to both cloud-size and precipitation-size particles. Its footprint is approximately 1.7 km along track and 1.3 km across track. The vertical resolution is 480 m, oversampled to 240 m. Stephens *et al.* [2008] provides an overview of the CloudSat data. Further details can be found from CloudSat Data Processing Center at <http://cloudsat.cira.colostate.edu>. In this study, we use 2B-GEOPROF data to estimate LNB_observation for deep convection. 2B-GEOPROF includes both radar reflectivity and cloud mask (cloud mask value ≥ 20 is used to identify clouds, which corresponds to reflectivity ~ -30 dBZ). Ambient soundings are taken from ECMWF-AUX product containing temperature and moisture profiles from the European Centre for Medium-Range Weather Forecast (ECMWF) operational analysis interpolated in space and time to the CloudSat track. Data from June 2006 through December 2008 are analyzed.

[8] The premise of this analysis is that cirrus anvils developing out of deep convection is a natural manifestation of where convection loses buoyancy and can thus be used as a proxy for LNB_observation. This gives us a clear feature of interest to search among cloud objects observed by CloudSat. Figure 1 shows an example with a number of

typical features readily identifiable: convective core is located near the center and overshoots above the rest of the cloud deck; cirrus anvils are well developed and expand horizontally.

[9] Here we briefly describe our cloud selection method. Analysis starts from screening of each cloud object, defined as the area enclosed by cloud mask > 20 in the CloudSat 2B-GEOPROF reflectivity data, similar to Riley and Mapes [2009] and Bacmeister and Stephens [2011]. Given the CloudSat “curtain-like” sampling, one can think of a cloud object as the vertical cross section of a three-dimensional cloud. For each cloud object, we first look for the presence of deep convective core (DCC), which is defined as a CloudSat profile having 1) continuous radar echo from cloud top to within 2 km of the surface (i.e., the target cloud is rooted in the planetary boundary layer), and 2) echo top height (ETH) of the 10 dBZ greater than 10 km. These criteria are broadly in line with the characteristics of active convective cores as observed in Luo *et al.* [2008]. Once the DCC is identified, we search horizontally on both sides of the cores for the attached anvils. Cloud base ≥ 5 km is required for anvils, following the statistics of the anvil base height in a previous study by Yuan and Houze [2010]. We further impose the condition that the horizontal span of the cirrus anvil must be greater than 20 km to insure that the anvil is well developed and that enough information is available for estimating LNB_observation. Requiring the existence of the DCC makes it more likely that the detrainment is still fresh, minimizing the effect of ice particle sedimentation which may introduce a lower bias to the estimated LNB_observation. A total of 4,008 suitable cloud objects are selected from 2.5 years of CloudSat data.

[10] For each selected convective objects, we define three forms of LNB_observation to capture the full range over

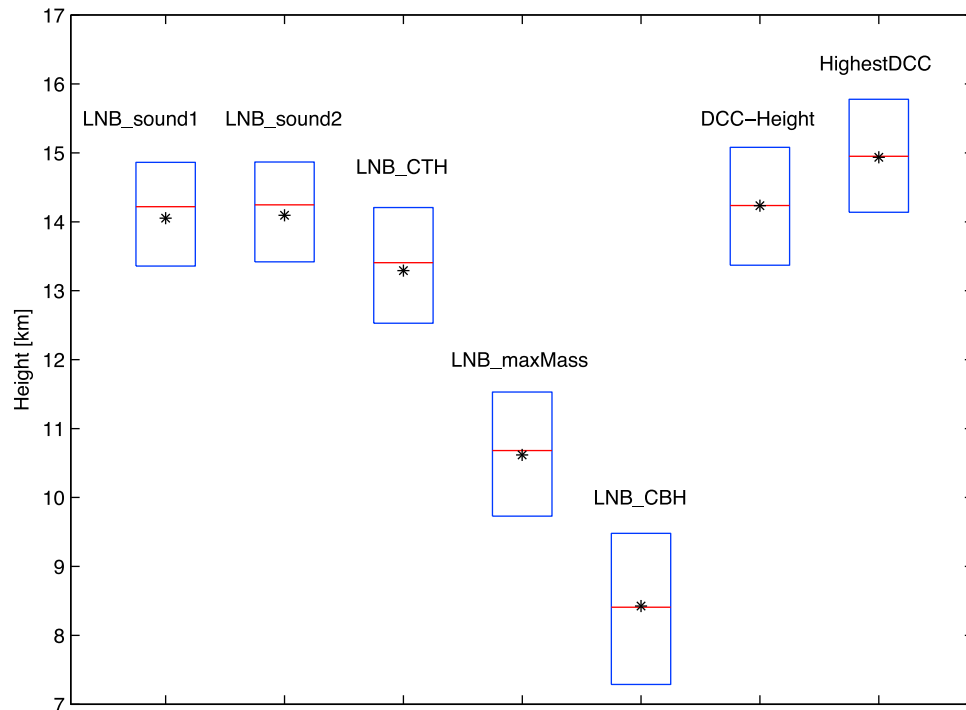


Figure 2. Box diagram for LNB_sounding, LNB_CTH, LNB_maxMass, LNB_CBH, height of DCC and of the highest point. The bottom and top of the boxes show, respectively, the 25% and 75% percentile. The central lines show the median and stars inside the box show the mean.

which convective detrainment develops: 1) LNB is first estimated from the cloud-top height (CTH) of the anvils, which we call LNB_CTH. This is the highest detrainment level and represents the destiny of the “lucky” parcels that are relatively less diluted during ascent or the ones that have the larger originating moist static energy in the planetary boundary layer. LNB_CTH can be readily compared to the infrared measurements, given the anvil is thick enough so that the infrared brightness temperature is representative of the cloud-top temperature. 2) Similarly, cloud base height (CBH) of the anvils is also estimated, referred to as the LNB_CBH. This is the lowest detrainment level and may come from the more diluted convective air parcels, or alternatively, the air parcels with lower originating moist static energy. LNB_CTH and LNB_CBH bracket the range of the effective LNB that can be determined observationally. 3) In between these two, we also estimate LNB using the height of the maximum radar reflectivity within the anvil column, which we call LNB_maxMass because *Mullendore et al.*'s [2009] case study shows that this level is well correlated with the maximum mass detrainment. LNB_maxMass is thus most relevant to convective mass transport.

[11] Figure 1 used an example to illustrate how various forms of LNB_observations are estimated. Multiple ways of defining the LNB_observations help capture the complex nature of convective detrainment. Together, they provide a more complete depiction of where convection loses buoyancy than IR data can do. For all the three forms of LNB_observations, calculation is done profile by profile first and then averaged over the first 20 km of the anvils. Choice of the first 20 km of the anvil is a compromise between the need to minimize random noises (longer samples preferred) and the concern of the bias due to ice sedimentation (shorter

distance from the DCC preferred). According to *Mullendore et al.*'s [2009] case study, ice particle sedimentation would introduce a vertical displacement of ~ 1.2 km when ice particles travel 20 km from the initial detraining point, assuming mean outflow speed of 5 m/s.

[12] LNB_sounding is calculated from the collocated ECMWF analysis profiles assuming pseudoadiabatic ascent from the planetary boundary layer. Given that the analysis tends to smooth out meteorological fields, we may expect some underestimation of LNB_sounding. However, the exact impact is difficult to quantify because of lack of collocated radiosonde data. We neglect the effect of hydrometeor loading and freezing. They tend to cancel each other: hydrometeor loading lowers LNB while latent heat of fusion increases LNB. *Emanuel* [1994] found a nearly exact cancellation using soundings over Florida in summer (their Figure 14.4). To account for the uncertainty associated with the originating level, we launch the air parcel from both the surface and the level having the maximum moist static energy (MSE) between the surface and 925 hPa, following *Liu and Zipser* [2005]. They are referred to as LNB_sounding1 and LNB_sounding2, respectively. LNB_sounding2 is by definition higher than LNB_sounding1, but our results show that the difference between them is usually small (average < 30 m) so in discussions we only use LNB_sounding2. Finally, since this study focuses on tropical deep convection, we exclude in our analysis cases that are occasionally found to have LNB_sounding < 10 km.

3. Results and Interpretations

[13] Figure 2 shows the statistics of LNB_sounding and various forms of LNB_observations based on analysis of 2.5

Table 1. Median Value (standard deviation) of LNB_Sounding, LNB_CTH, LNB_maxMass, LNB_CBH, DCC Height, the Highest Point of DCC (unit: m), and Size of DCC and of the Whole System (unit: km), as well as the Total Number of Selected Convective Cloud Objects

Median (STD)	LNB_sounding1	LNB_sounding2	LNB_CTH	LNB_maxMass	LNB_CBH
All	14,219 (1,203)	14,247 (1,163)	13,406 (1,365)	10,680 (1,342)	8,409 (1,495)
Ocean	14,229 (1,141)	14,234 (1,135)	13,293 (1,358)	10,548 (1,315)	8,272 (1,473)
Land	14,185 (1,388)	14,268 (1,254)	13,756 (1,327)	11,141 (1,337)	8,783 (1,527)
Median (STD)	DCC-Height	Highest DCC	System Size	DCC Size	Number of Cases
All	14,237 (1,194)	14,951 (1,204)	159.5 (159.7)	11 (25.7)	4008
Ocean	14,125 (1,168)	14,841 (1,186)	167.2 (165.1)	9.9 (25.1)	3087
Land	14,654 (1,198)	15,373 (1,176)	139.7 (136.5)	14.3 (27.5)	909

years of CloudSat data. Also included are the statistics for the DCC heights and the highest point of the cores. Several findings deserve discussion. 1) LNB_CTH Vs LNB_sounding: LNB_CTH is slightly lower than LNB_sounding: the median values for LNB_CTH and LNB_sounding are, respectively, 13.41 km and 14.25 km. This suggests that LNB determined by the ambient sounding provides an overall reasonable upper bound for the convective development. However, there is little one-to-one correspondence between LNB_sounding and LNB_CTH (both LNB_sounding and LNB_CTH span a large range from 10 to 16 km) as the linear correlation between them is only 0.29 (0.30 over ocean and 0.28 over land). So, although setting a reasonable upper limit, ambient sounding contains limited information content to accurately predict the height where actual convective clouds lose buoyancy and detrain mass. 2) LNB_maxMass Vs LNB_sounding: The median value of LNB_maxMass (10.68 km) is more than 3 km lower than that of LNB_sounding (14.25 km). Recall that LNB_maxMass measures the level where maximum mass detrainment occurs. This means that the majority of the convective air parcels lose their buoyancy at a level that is considerably lower than that set by the ambient sounding. From convective transport perspective, LNB_sounding is a significant overestimate of the “destination” height level of the detrained mass. The correlation between LNB_sounding and LNB_maxMass is 0.28 (0.30 over ocean and 0.25 over land), which again points to the limited value of using LNB_sounding to predict LNB_maxMass on a case-by-case basis. 3) LNB_CBH Vs LNB_sounding: LNB_CBH is further lower; the median value is only 8.41 km. Correlation between LNB_sounding and LNB_CBH is only 0.20 (0.21 over ocean and 0.16 over land). LNB_CTH (13.41 km) and LNB_CBH (8.41 km) bracket the height range over which tropical deep convection develops outflow and detrains mass.

[14] Figure 2 also shows that convective cores with the median height of 14.24 km generally overshoot the level set by LNB_CTH (13.41 km). The median value of the highest point of the DCCs reaches 14.95 km. These height levels associated with the cores are higher than the base of the tropical tropopause layer (TTL), which is generally considered as located at ~ 14 km [Fueglistaler *et al.*, 2009]. Hence, our results suggest that the DCCs have the potential to directly participate in the stratosphere-troposphere exchange, while the anvils with the median top height at 13.41 km are mainly confined within the troposphere.

[15] Some land-ocean differences are observed (Table 1). We first note that LNB_sounding is very similar between

land (median: 14.27 km) and ocean (median: 14.23 km). However, all three forms of LNB_observations are higher over land than over ocean: the median values for land (ocean) LNB_CTH, LNB_maxMass, and LNB_CBH are, respectively, 13.76 km (13.29 km), 11.14 km (10.55 km), and 8.78 km (8.27 km). Student’s *t*-test confirms that all the differences are statistically significant at 0.95 confidence level. So, outflow from land deep convection pushes closer to the height level set by the ambient sounding than the oceanic counterpart. This may be related to the land-ocean difference in convective intensity [e.g., Zipser *et al.*, 2006]: stronger updrafts in land convection may bring the ascending air parcels to greater altitude and detrain mass at a higher level.

[16] In addition to the vertical dimension, land and ocean deep convection also exhibits some difference in horizontal size. From CloudSat radar data, we define the size of a cloud object as the horizontal span of the CloudSat profiles, following that by Luo *et al.* [2011]. The median size of the land convective systems (including both anvils and cores) is 140 km and that of the ocean counterpart is 167 km. On the contrary, median size of the DCCs shows the opposite trend: 14 km for land convection and 10 km for ocean convection. Both differences are statistically significant at 0.95 confidence level. Although our definition of cloud size is somewhat different from previous studies using passive sensors (e.g., IR images), a qualitative comparison can still be made. A number of publications have shown that convective system over ocean is larger than over land. For example, Machado and Rossow [1993] arrived at this conclusion by conducting a global analysis of tropical cold cloud cluster (spatially-adjacent pixels in IR images with cloud-top temperature colder than 245 K). On the other hand, larger cores for land convection than ocean convection have been documented in studies using precipitation radar [e.g., Liu *et al.*, 2007] and *in situ* aircraft measurements [e.g., Lucas *et al.*, 1994]. Analysis of CloudSat data corroborate these previous work and further establish the fact that oceanic convective systems are bigger but the embedded convective cores are narrower.

[17] The final “fate” of the updraft air parcels is closely related to their interaction with the environment. For example, entrainment of ambient air with lower moist static energy can significantly lower the effective LNB of these ascending air parcels. The difference between LNB_observation and LNB_sounding may thus be interpreted as a measure of the magnitude of the entrainment effect: the greater the entrainment rate, the larger the height difference. Here, we use a simple model (entraining plume model) to understand the

differences between LNB_sounding and LNB_observation. Despite the simplified form, the entraining plume model is commonly used in GCM cumulus parameterization schemes in which cumulus convection is modeled as an ensemble of plumes with characteristic LNB and entrainment rates, each sharing a fraction of the total convective mass fluxes as determined by the parameterization's closure scheme [e.g., Arakawa and Schubert, 1974]. As observational equivalents, we may regard LNB_CTH, LNB_maxMass and LNB_CBH as representing the final outflow destination of three general types of "plumes": LNB_CTH (LNB_CBH) corresponds to the highest (lowest) reaching plume with the smallest (largest) entrainment rate and LNB_maxMass to the plume that has the largest share of the deep convective mass flux.

[18] Following Luo *et al.* [2010], the entraining plume model is formulated as: $\frac{\partial MSE_p}{\partial z} = \lambda(MSE_e - MSE_p)$, where λ is the bulk entrainment rate (unit: %/km), and moist static energy (MSE) $\equiv C_p T + gz + L_v q$ (T , z and q are temperature, height and specific humidity, respectively; C_p is the specific heat of dry air, g gravitational acceleration, and L_v the latent heat of condensation); subscripts p and e refer to properties of the in-cloud air parcel and of the environment, respectively. MSE_e can be estimated from the sounding data. We calculate λ iteratively by integrating the equation from the surface to the corresponding LNB_observation. The calculated mean bulk entrainment rates for LNB_CTH, LNB_maxMass, and LNB_CBH are, respectively, 3%/km, 6%/km and 10%/km. These numbers are in the similar range of the estimates given by Luo *et al.* [2010] for tropical deep convection. They may serve as an observational constraint for adjusting GCM cumulus parameterizations. For example, a recent study by Kim *et al.* [2011] showed that an improved simulation of ENSO variability can be achieved by setting a minimum allowable entrainment rate. Our results give some observational guidance concerning what minimum thresholds to choose.

[19] There are also some land-ocean differences. The mean entrainment rates are slightly smaller over land than over ocean. For example, the corresponding entrainment rates for land (ocean) LNB_maxMass and LNB_CBH are, respectively, 6%/km (7%/km), and 9%/km (10%/km). This difference may be attributable to the size difference of convective cores: land convection tends to have larger convective cores, which provide better protection from entrainment dilution [Lucas *et al.*, 1994]. Our analysis of the DCC width supports this explanation (Table 1).

4. Summaries and Discussion

[20] This study revisits an old concept in meteorology – level of neutral buoyancy (LNB). The classic definition of LNB follows the parcel theory assuming no dilution by the surroundings; it can be simply derived from the ambient sounding (LNB_sounding). In reality, however, convection interacts with the environment in complicated ways. It will eventually find its own effective LNB and manifests it through detraining masses and developing anvils (LNB_observation). In this study, we conduct a near-global survey of LNB_observation for tropical deep convection using CloudSat data and make comparison with the corresponding LNB_sounding. Three forms of LNB_observation are defined to reflect the fact that convective detraining occurs over a broad range of heights: LNB_CTH refers to the highest detraining

level, LNB_CBH the lowest detraining level, and LNB_maxMass corresponds to the level of maximum mass detraining. The principal findings are as follows:

[21] 1. LNB_sounding provides an overall reasonable upper bound for convective development. However, linear correlation between LNB_sounding and LNB_CTH is only 0.29, suggesting that ambient sounding alone contains limited information content to accurately predict the actual LNB where convective clouds lose buoyancy and detraining mass.

[22] 2. LNB_maxMass, which measures the level of maximum mass detraining, is more than 3 km lower than LNB_sounding. So, LNB_sounding is a significant overestimate of the "destination" of convective mass transport. Correlation between LNB_maxMass and LNB_sounding is only 0.28.

[23] 3. All three forms of LNB_observation are higher over land than over ocean, while LNB_sounding is very similar between land and ocean. So, deep convection over land tends to detraining mass at a higher level and the outflow from land convection pushes closer to the height level set by the ambient sounding. Moreover, it is noticed that oceanic deep convective systems are larger than their land counterparts, but the embedded convective cores in the oceanic systems are smaller.

[24] 4. The difference between LNB_sounding and LNB_observation is closely related to convective entrainment because entraining ambient air with lower moist static energy will lower the LNB_observation. Using an entraining plume model, we estimate the bulk entrainment rates (λ) associated with all three forms of LNB_observation: the mean λ values for LNB_CTH, LNB_maxMass and LNB_CBH are, respectively, 3%/km, 6%/km and 10%/km. The estimated entrainment rates can serve as observational constraints for adjusting GCM cumulus parameterization.

[25] **Acknowledgments.** The study was supported by two NASA grants awarded to CUNY: NNX10AM31G and NNX12AC13G. The authors would like to thank William Rossow, Susan van den Heever and Ed Zipser for insightful discussions.

[26] The Editor thanks the two anonymous reviewers for assisting in the evaluation of this paper.

References

- Arakawa, A., and W. H. Schubert (1974), Interaction of a cumulus cloud ensemble with the large scale environment. Part I, *J. Atmos. Sci.*, *31*, 674–701, doi:10.1175/1520-0469(1974)031<0674:IOACCE>2.0.CO;2.
- Bacmeister, J. T., and G. L. Stephens (2011), Spatial statistics of likely convective clouds in CloudSat data, *J. Geophys. Res.*, *116*, D04104, doi:10.1029/2010JD014444.
- Bedka, K., J. Brunner, R. Dworak, W. Feltz, J. Otkin, and T. Greenwald (2010), Objective satellite-based detection of overshooting tops using infrared window channel brightness temperature gradients, *J. Appl. Meteorol. Climatol.*, *49*, 181–202.
- Cetrone, J., and R. A. Houze Jr. (2009), Anvil clouds of tropical mesoscale convective systems in monsoon regions, *Q. J. R. Meteorol. Soc.*, *135*, 305–317, doi:10.1002/qj.389.
- Emanuel, K. A. (1994), *Atmospheric Convection*, 580 pp., Oxford Univ. Press, Oxford, U. K.
- Fueglistaler, S., A. E. Dessler, T. J. Dunkerton, I. Folkins, Q. Fu, and P. W. Mote (2009), Tropical tropopause layer, *Rev. Geophys.*, *47*, RG1004, doi:10.1029/2008RG000267.
- Kim, D., Y.-S. Jang, D.-H. Kim, Y.-H. Kim, M. Watanabe, F.-F. Jin, and J.-S. Kug (2011), El Niño–Southern Oscillation sensitivity to cumulus entrainment in a coupled general circulation model, *J. Geophys. Res.*, *116*, D22112, doi:10.1029/2011JD016526.
- Li, W., and C. Schumacher (2011), Thick anvils as viewed by the TRMM Precipitation Radar, *J. Clim.*, *24*, 1718–1735, doi:10.1175/2010JCLI3793.1.

- Liu, C., and E. J. Zipser (2005), Global distribution of convection penetrating the tropical tropopause, *J. Geophys. Res.*, *110*, D23104, doi:10.1029/2005JD006063.
- Liu, C., E. J. Zipser, and S. W. Nesbitt (2007), Global distribution of tropical deep convection: Different perspectives from TRMM infrared and radar data, *J. Clim.*, *20*, 489–503, doi:10.1175/JCLI4023.1.
- Lucas, C., M. A. LeMone, and E. J. Zipser (1994), Vertical velocity in oceanic convection off tropical Australia, *J. Atmos. Sci.*, *51*, 3183–3193, doi:10.1175/1520-0469(1994)051<3183:VVIOCO>2.0.CO;2.
- Luo, Z., G. Y. Liu, and G. L. Stephens (2008), CloudSat adding new insight into tropical penetrating convection, *Geophys. Res. Lett.*, *35*, L19819, doi:10.1029/2008GL035330.
- Luo, Z. J., G. Y. Liu, and G. L. Stephens (2010), Use of A-Train data to estimate convective buoyancy and entrainment rate, *Geophys. Res. Lett.*, *37*, L09804, doi:10.1029/2010GL042904.
- Luo, Y., R. Zhang, W. Qian, Z. Luo, and X. Hu (2011), Intercomparison of deep convection over the Tibetan Plateau-Asian monsoon region and subtropical North America in boreal summer using CloudSat/CALIPSO data, *J. Clim.*, *24*, 2164–2177, doi:10.1175/2010JCLI4032.1.
- Machado, L. A. T., and W. B. Rossow (1993), Structural characteristics and radiative properties of tropical cloud clusters, *Mon. Weather Rev.*, *121*, 3234–3260, doi:10.1175/1520-0493(1993)121<3234:SCARPO>2.0.CO;2.
- Mullendore, G. L., A. J. Homann, K. Bevers, and C. Schumacher (2009), Radar reflectivity as a proxy for convective mass transport, *J. Geophys. Res.*, *114*, D16103, doi:10.1029/2008JD011431.
- Riley, E. M., and B. E. Mapes (2009), Unexpected peak near -15°C in CloudSat echo top climatology, *Geophys. Res. Lett.*, *36*, L09819, doi:10.1029/2009GL037558.
- Stephens, G. L., et al. (2008), CloudSat mission: Performance and early science after the first year of operation, *J. Geophys. Res.*, *113*, D00A18, doi:10.1029/2008JD009982.
- Yuan, J., and R. A. Houze Jr. (2010), Global variability of mesoscale convective system anvil structure from A-Train satellite data, *J. Clim.*, *23*, 5864–5888, doi:10.1175/2010JCLI3671.1.
- Yuan, J., R. A. Houze Jr., and A. J. Heymsfield (2011), Vertical structures of anvil clouds of tropical mesoscale convective systems observed by CloudSat, *J. Atmos. Sci.*, *68*, 1653–1674, doi:10.1175/2011JAS3687.1.
- Zipser, E. J., et al. (2006), Where are the most intense thunderstorms on Earth?, *Bull. Am. Meteorol. Soc.*, *87*, 1057–1071, doi:10.1175/BAMS-87-8-1057.